

## Turbulence and Multiscaling in the Randomly Forced Navier-Stokes Equation

Anirban Sain,<sup>1</sup> Manu,<sup>2,\*</sup> and Rahul Pandit<sup>1,†</sup>

<sup>1</sup>Department of Physics, Indian Institute of Science, Bangalore 560 012, India

<sup>2</sup>School of Physical Sciences, Jawaharlal Nehru University, New Delhi 110 067, India

(Received 29 December 1997)

We present a pseudospectral study of the randomly forced Navier-Stokes equation (RFNSE) stirred by a stochastic force with zero mean and a variance  $\sim k^{4-d-y}$ , with  $k$  the wave vector and the dimension  $d = 3$ . We provide the first evidence for multiscaling of velocity structure functions for  $y \geq 4$ . We extract the multiscaling exponent ratios  $\zeta_p/\zeta_2$  by using extended self-similarity, examine their dependence on  $y$ , and show that, if  $y = 4$ , they are in agreement with those obtained for the Navier-Stokes equation forced at large spatial scales (3DNSE). Also well-defined vortex filaments, which appear clearly in studies of the 3DNSE, are absent in the RFNSE. [S0031-9007(98)07657-1]

PACS numbers: 47.27.Eq, 05.45.+b, 05.70.Jk, 47.27.Gs

Kolmogorov's classic work (K41) on homogeneous, isotropic fluid turbulence focused on the scaling behavior of velocity  $\mathbf{v}$  structure functions  $S_p(r) = \langle |\mathbf{v}_i(\mathbf{x} + \mathbf{r}) - \mathbf{v}_i(\mathbf{x})|^p \rangle$ , where the angular brackets denote an average over the statistical steady state [1]. He suggested that, for separations  $r \equiv |\mathbf{r}|$  in the *inertial range*, which is substantial at large Reynolds numbers  $Re$  and lies between the forcing scale  $L$  and the dissipation scale  $\eta_d$ , these structure functions scale as  $S_p \sim r^{\zeta_p}$ , with  $\zeta_p = p/3$ . Subsequent experiments [2] have suggested instead that multiscaling obtains with  $p/3 > \zeta_p$ , which turns out to be a nonlinear, monotonically increasing function of  $p$ ; this has also been borne out by numerical studies of the three-dimensional Navier-Stokes equation forced at large spatial scales (3DNSE) [2,3]. The determination of the exponents  $\zeta_p$  has been one of the central, but elusive, goals of the theory of turbulence. One of the promising starting points for such a theory is the randomly forced Navier-Stokes equation (RFNSE) [4–6], driven by a Gaussian random force whose spatial Fourier transform  $\mathbf{f}(\mathbf{k}, t)$  has zero mean and a covariance  $\langle \mathbf{f}_i(\mathbf{k}, t) \mathbf{f}_j(\mathbf{k}', t') \rangle = Ak^{4-d-y} P_{ij}(\mathbf{k}) \delta(\mathbf{k} + \mathbf{k}') \delta(t - t')$ ; here  $\mathbf{k}, \mathbf{k}'$  are wave numbers,  $t, t'$  times,  $i, j$  Cartesian components in  $d$  dimensions, and  $P_{ij}(\mathbf{k})$  the transverse projector which enforces the incompressibility condition. One-loop renormalization-group (RG) studies of this RFNSE yield [4,5] a K41 energy spectrum, namely,  $E(k) \sim k^2 S_2(k) \equiv k^2 \langle |\mathbf{v}(\mathbf{k})|^2 \rangle \sim k^{-5/3}$ , if we set  $d = 3$  and  $y = 4$ ; this has also been verified numerically [6]. Nevertheless, these RG studies have been criticized for a variety of reasons [7,8] such as using a large value for  $y$  in a small- $y$  expansion and neglecting an infinity of marginal operators (if  $y = 4$ ). These criticisms of the *approximations* used in these studies might well be justified, but they clearly cannot be used to argue that the RFNSE is *in itself* inappropriate for a theory of turbulence. It is our purpose here to test whether structure functions in the RFNSE display the same multiscaling as in the 3DNSE for some value of  $y$ ; if so, then the RFNSE can, defensibly,

be used to develop a statistical theory of inertial-range multiscaling in homogeneous, isotropic fluid turbulence.

We have carried out an extensive pseudospectral study of the RFNSE and compared our results with earlier numerical studies [3,9] of the 3DNSE and experiments [2]. We find several interesting and new results: We show that structure functions in the RFNSE display multiscaling for  $y \geq 4$ . We obtain  $\zeta_2$  from  $S_2(k)$  (Fig. 1) and the exponent ratios  $\zeta_p/\zeta_2$  by using the extended-self-similarity (ESS) procedure (Fig. 2a) [9,10]. We find that  $\zeta_p/\zeta_2$  is close to the 3DNSE result (Fig. 2b) for  $y = 4$  at least for  $p \leq 7$ . Furthermore we show that the qualitative behaviors of the probability distributions  $P(\delta v_\alpha(r))$ , where  $\delta v_\alpha(r) \equiv v_\alpha(\mathbf{x}) - v_\alpha(\mathbf{x} + \mathbf{r})$ , are similar in the two models (Fig. 2c), but the shapes of constant- $|\omega|$

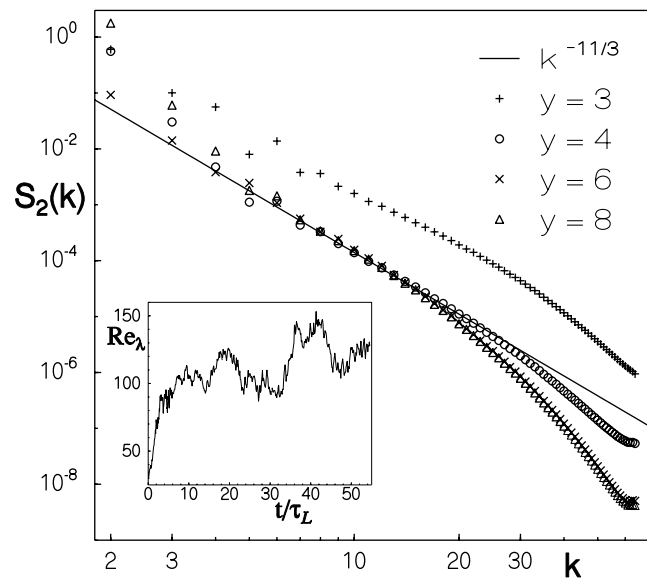


FIG. 1. Log-log plots (base 10) of  $S_2(k)$  versus  $k$  for different values of  $y$ . The line indicates the K41 result  $S_2(k) \sim k^{-11/3}$ .  $\mathbf{k}$  indicates the shell number, which is twice the wave number ( $= \frac{2\pi}{L} n$ ). The inset shows a representative plot of  $Re_\lambda$  versus time ( $t$ ) for  $y = 4$ .

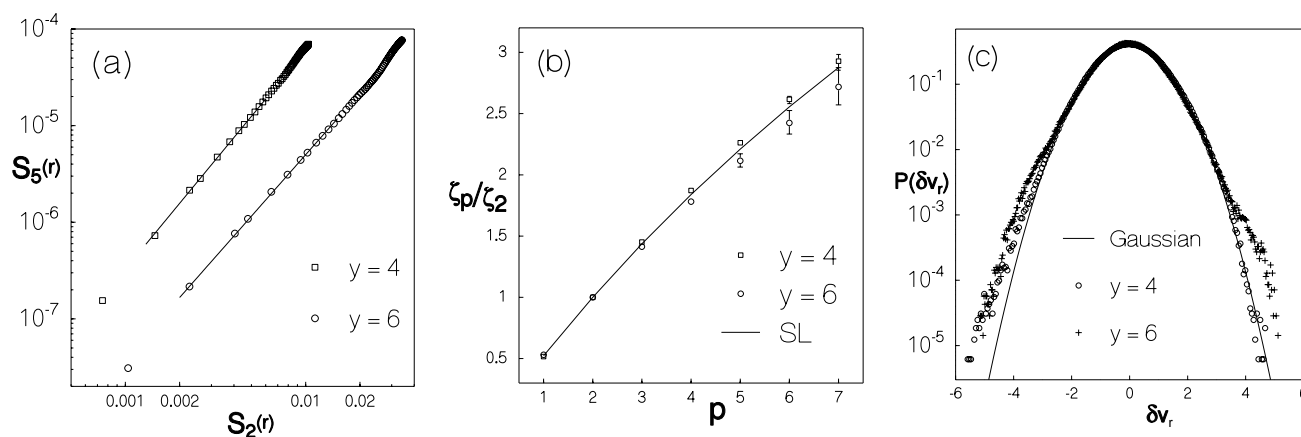


FIG. 2. (a) Log-log plots (base 10) of  $S_5(r)$  versus  $S_2(r)$  illustrating the ESS procedure; full lines indicate fits to points in the extended inertial range; (b) inertial-range exponent ratios  $\zeta_p/\zeta_2$  versus  $p$  for the RFNSE with  $y = 4$  and  $6$  [extracted from plots such as (a)]; the line indicates the SL formula; (c) semilog plots of the distribution  $P(\delta v_r)$  [i.e.,  $P(\delta v_\alpha(r))$  averaged over  $\alpha$  for  $r$  in the dissipation range and  $y = 4$  and  $6$ ]; a Gaussian distribution is shown for comparison.

surfaces, where  $\omega$  is the vorticity, are markedly different (Fig. 3); the stochastic force destroys well-defined filamentary structures that obtain in 3DNSE studies. This has implications for the She-Leveque (SL) [11] formula for  $\zeta_p$  as we discuss below.

We use a pseudospectral method [12] to solve the RFNSE numerically on a  $64^3$  grid with a cubic box of linear size  $L = 2\pi$  and periodic boundary conditions; we have checked in representative cases that our results are unchanged if we use an  $80^3$  grid or aliasing. Aside from the stochastic forcing [13], our numerical scheme is the same as in Ref. [9]. Our dissipation term,  $(\nu + \nu_H k^2)k^2 \mathbf{v}(\mathbf{k})$  in wave-vector ( $k$ ) space, includes both the viscosity  $\nu$  and the hyperviscosity  $\nu_H$ ; the exponents  $\zeta_p$  are unaffected by  $\nu_H$  if  $\nu > 0$  [9,14]. For a fixed grid size we can attain higher Taylor-microscale Reynolds numbers  $Re_\lambda$  in the RFNSE, and hence a larger inertial range, than in the 3DNSE ( $Re_\lambda \approx 120$  compared to  $Re_\lambda \approx 22$  in our study), as noted earlier [6] for  $y = 4$ . This advantage is reduced somewhat by the need to aver-

age statistical observables longer in the RFNSE than in the 3DNSE. In the latter case it normally suffices to average over a few box-size eddy turnover times  $\tau_L$ ; this is not enough for the RFNSE since (a)  $Re_\lambda$  fluctuates strongly over time scales considerably larger than  $\tau_L$  (inset in Fig. 1) and (b) the length of the  $\mathbf{f}(\mathbf{k}, t)$  time series required to obtain a specified variance for the stochastic force is quite large ( $\approx 6\tau_L$  to achieve the given variance within 1%–2%). We have collected data for averages over  $(25\text{--}33)\tau_L$  (for different values of  $y$ ), after initial transients have been allowed to decay [over times  $\approx (10\text{--}20)\tau_L$ ]. Our  $\tau_L \approx 10\tau_I$ , the integral-scale time used in some studies [12];  $\tau_I \equiv L_I/\nu_{rms}$ , where the integral scale  $L_I \equiv [\int dk k E(k)/\int dk E(k)]^{-1}$  and  $\nu_{rms}$  is the root-mean-square velocity. We have checked explicitly that the RFNSE captures the hierarchy of time scales present in the 3DNSE. In spite of the delta-correlated stochastic force in the RFNSE, the variation of  $\mathbf{v}(\mathbf{k})$  as a function of time is similar in both the RFNSE and the 3DNSE: There is a hierarchy of time scales which increase with decreasing  $k \equiv |\mathbf{k}|$ . In the RFNSE, the stochastic force puts a high-frequency ripple on  $\mathbf{v}(\mathbf{k})$  even for small  $k$ , but this does not affect its overall variation significantly, nor does it affect the multiscaling exponent ratios if  $y = 4$ , as we show below.

We begin by investigating the inertial-range scaling of the  $k$ -space structure function  $S_2(k) \sim k^{-\zeta'_2}$ . Given this power-law form, the exponent  $\zeta'_2$  is easily related to the  $r$ -space exponent  $\zeta_2$  by  $\zeta_2 = \zeta'_2 - 3$ . Our data in Fig. 1 for  $4 \leq y$  are consistent with  $\zeta'_2 = 11/3$  [i.e., the K41 value since  $E(k) \sim k^2 S_2(k) \sim k^{-5/3}$ ]. For  $y = 4$  this result has been reported earlier [6]. The  $y$  independence of  $\zeta'_2$  above some critical  $y_c$  [our data for  $S_2(k)$  suggest  $y_c \approx 4$ ] is theoretically satisfying since the variance of the stochastic force in the RFNSE rises rapidly at small  $k$ , so we might expect that, for sufficiently large  $y$ , it approximates the conventional forcing of the 3DNSE at large spatial scales. This has been explored in the  $N \rightarrow \infty$

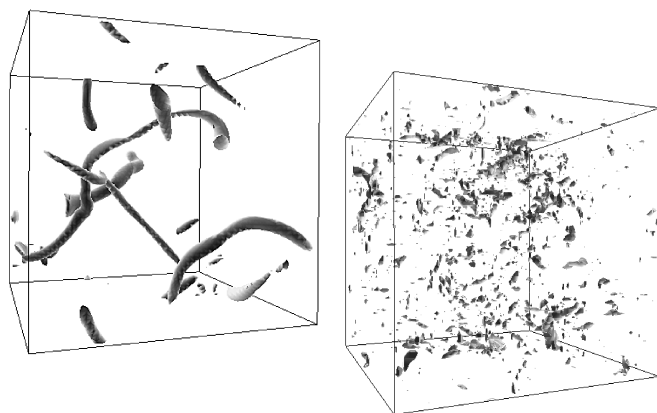


FIG. 3. Iso- $|\omega|$  surfaces obtained from instantaneous snapshots of the vorticity fields showing filaments for the 3DNSE (left) and no filaments for the RFNSE with  $y = 4$  (right).

limit of an  $N$ -component RFNSE [7]. This study suggests  $\zeta_2' = 7/2$  for  $y \geq y_c = 4$ ; given our error bars (Table I) it is difficult to distinguish this from the  $O(y)$  RG prediction  $\zeta_2' = 11/3$  though our data are closer to the latter. For  $0 < y \leq 3$  both the one-loop RG [5] and the  $N \rightarrow \infty$  theory [7] predict  $\zeta_2' \sim 1 + 2y/3 + O(y^2)$ , in fair agreement with our numerical results, especially for small  $y$  (Table I). Note that, for  $0 < y < 4$ , there is no *invariant* energy cascade as in conventional K41: The dominance of dissipation at large  $k$  does lead to an energy cascade, but the energy flux depends on the length scale  $r$ ; specifically  $\Pi(r) \approx Ar^{y-4}$ , with  $A$  the scale-independent part of the variance of the stochastic force. A K41-type argument [15] now yields an energy-transfer rate  $\sim \langle \delta v_r^3 \rangle / r \sim r^{(y-4)}$ , whence  $S_3(r) \sim r^{(y-3)}$  and, if we assume simple scaling as in K41,  $S_2(r) \sim r^{(y-3)2/3}$ , i.e.,  $\zeta_2' = 1 + 2y/3$ , as in the  $O(y)$  RG prediction. This formula breaks down for  $y < 0$ ; however, the RG predicts correctly that the linear-hydrodynamics result obtains in this regime.

We ensure that systematic errors do not affect  $\zeta_2'$  as follows. If  $k_{\max}$  is the largest wave-vector magnitude in our numerical scheme, we find that  $L_I k_{\max}$  decreases with decreasing  $y$ ; this shortens the inertial range which can be used to obtain  $\zeta_2'$ . The lower the value of  $y$  the more difficult it is to obtain a dissipation range free of finite-resolution errors. For  $y < 4$ , we define  $k_d \equiv \eta_d^{-1}$  to be the inverse length scale at which the energy-transfer time  $t_r \sim (r/\nu_r) \sim [Ar^{(y-6)}]^{1/3}$  equals the diffusion time  $t_D \sim [\nu k^2 + \nu_H k^4]^{-1}$ ; this yields  $\nu_0 k_d^2 + \nu_H k_d^4 = [Ak_d^{6-y}]^{1/3}$ , which when solved numerically shows that, for fixed  $A$ ,  $k_d$  increases as  $y$  decreases (in Table I  $A$  is not fixed). Statistical steady states, with ill-resolved dissipation ranges that do not have a decaying tail [9], can be obtained by adjusting  $A$ . In such cases  $k_d \gg k_{\max}$  and we get spurious results for  $\zeta_2'$ . We find that, if we increase the hyperviscosity  $\nu_H$ ,  $k_d$  is sufficiently close to  $k_{\max}$  so that we can resolve both inertial and dissipation ranges and obtain reliable values for  $\zeta_2'$ . Table I shows the range over which we fit our data for  $S_2(k)$ . Since our data for  $\zeta_2'$  indicate that  $y_c \approx 4$ , we investigate multiscaling only for  $y \geq 4$ .

Our data for  $\zeta_2'$  in Table I suggest that naive estimates for the  $\zeta_p$  require longer inertial ranges than are available in our studies. However, we find that, as in the 3DNSE, the extended-self-similarity procedure [3,9,10] can be used fruitfully here to extract the exponent ratios

$\zeta_p/\zeta_q$  from the slopes of log-log plots of  $S_p(r)$  versus  $S_q(r)$  (see Fig. 2) since this extends the apparent inertial range. We compare the resulting  $\zeta_p/\zeta_2$  in Fig. 2b with the She-Leveque formula [11], which provides a convenient parametrization for the experimental values for  $\zeta_p$ . Figure 2b shows that, with  $y = 4$ , our RFNSE exponent ratios lie very close to those for the 3DNSE and, to this extent, these two models are in the same *universality class*. We obtained  $\zeta_p/\zeta_2$  by a regression fit. We have also checked that a local-slope analysis of ESS plots like Fig. 2a yields exponent ratios nearly indistinguishable from those shown in Fig. 2b. The error bars in Fig. 2b give a rough estimate of the systematic error associated with the choice of the precise range of points which fall in the extended inertial range; they were obtained by varying the number of points used in our regression fits. The exponent ratios for  $y < 4$  lie away from the 3DNSE values. One might expect naively that, at very large values of  $y$ , the inertial-range behaviors of structure functions of all orders should be the same as in the 3DNSE. However, strictly speaking, this is not obvious *a priori*, neither from renormalization-group calculations [4,5,8] nor from  $N \rightarrow \infty$  calculations [7]. The former are not very helpful for large  $y$  since an infinity of marginal operators appears at  $y = 4$ ; all these become relevant for  $y > 4$ . The  $N \rightarrow \infty$  studies have been restricted to  $p = 2$ . For  $p > 3$ , our data for  $\zeta_p/\zeta_2(y = 6)$  fall systematically below those for  $\zeta_p/\zeta_2(y = 4)$  or the SL line. Also the probability distributions of  $P(\delta v_r)$  (Fig. 2c) have non-Gaussian tails for  $r$  in the dissipation range, and for  $y > 4$  the deviations from a Gaussian distribution increase systematically with  $y$ . Thus, at the resolution of our calculation, the RFNSEs with  $y = 4$  and  $y = 6$  are in different universality classes. However, we point out that our data for  $y = 6$  are more noisy and yield a smaller inertial range ( $k_d \approx 20$ ) than those for  $y = 4$  (Table I). So longer runs with finer grids might well be required to settle this issue conclusively.

Strictly speaking the RFNSE with  $y = 4$  falls in the same universality class as the 3DNSE only in the ESS sense. For arbitrary  $y$  the energy flux through the  $k$ th shell is  $\Pi_k \equiv \Pi(r = k^{-1}) \sim \int_{1/L}^k \langle |\mathbf{f}(\mathbf{k})|^2 \rangle d^3k$ , where  $r$  is in the inertial range and we have used Novikov's theorem [15], i.e.,  $\langle \mathbf{f}(\mathbf{k}) \cdot \mathbf{v}(-\mathbf{k}) \rangle \sim \langle |\mathbf{f}(\mathbf{k})|^2 \rangle$ . For  $y > 4$ ,  $\Pi_k$  saturates to a constant for  $kL \gg 1$ , but for  $y = 4$ ,  $\Pi_k \sim \log(kL)$  in the RFNSE [16]. This is to be

TABLE I. The dissipation-scale wave number  $k_d$  (see text), the integral-scale wave number  $k_I \equiv L_I^{-1}$ , the apparent inertial range over which we fit our data for  $S_2(k)$ , the hyperviscosities  $\nu_H$ , the exponent  $\zeta_2'$  that we compute, and its  $O(y)$  RG value, for  $1 \leq y \leq 4$ . The viscosity  $\nu$  is  $5 \times 10^{-4}$  in all these runs which use a  $64^3$  grid.

$y$	$k_d$	$k_I$	Fitting range	$\nu_H$	$\zeta_2'$ (This study)	$\zeta_2'$ from $O(y)$ RG
4	49.0	1.16	$(0.1-0.5)k_d$	$10^{-6}$	$3.6 \pm 0.1$	$\approx 3.67$
3	38.7	1.90	$(0.16-0.52)k_d$	$3 \times 10^{-6}$	$3.0 \pm 0.1$	$\approx 3$
2	35.0	5.90	$(0.17-0.63)k_d$	$8 \times 10^{-6}$	$2.3 \pm 0.1$	$\approx 2.33$
1	35.4	10.3	$(0.2-0.7)k_d$	$8 \times 10^{-6}$	$1.6 \pm 0.15$	$\approx 1.67$

contrasted with the 3DNSE where  $\Pi_k = \text{const.}$  Thus the inertial-range behaviors of all correlation functions in the two models are not the same. A K41-type dimensional analysis suggests that for  $y = 4$  the energy flux  $\Pi_k \sim \langle \delta v_r^3 \rangle / r \sim \log(r/L)$ ; if we assume that there is no multiscaling, then  $S_p(r) \sim [r \log(r/L)]^{p/3}$ . Multiscaling will clearly modify this simple prediction, but some weak deviation from the von Karman–Howarth form  $S_3(r) \sim r$  must remain, since the standard derivation of this relation [15] does not go through [17] with the RFNSE result for  $\Pi_k$ . Since our data show that the ESS procedure works for the RFNSE, these weak deviations must cancel in the ratios of structure functions, and, as noted above, for  $y = 4$  the  $\zeta_p/\zeta_2$  agree with the SL result for the 3DNSE.

Filamentary structures (Fig. 3) [18] in iso- $|\omega|$  plots are important in phenomenological models for multiscaling in fluid turbulence. For example, the SL formula [11] is obtained by postulating a hierarchical relation among the moments of the scale-dependent energy dissipation; this yields a difference equation for the exponents  $\tau_p$ , which are simply related to the exponents  $\zeta_p$ ; one of the crucial boundary conditions used to solve this equation requires the codimension of the most intense structures. If these are taken to be vorticity filaments, their codimension is 2 and one gets the SL formula. Filaments have been observed in experiments also [19]. We have shown above that the exponent ratios  $\zeta_p/\zeta_2$  that we obtain from the RFNSE with  $y = 4$  agree with the SL formula. One might expect, therefore, that filamentary structures should appear in iso- $|\omega|$  plots for the RFNSE. However, this is not the case as can be seen from the representative plot shown in Fig. 3. The stochastic forcing seems to destroy the well-defined filaments observed in the 3DNSE *without changing the multiscaling exponent ratios*. Therefore, the existence of vorticity filaments is not crucial for obtaining these exponents, which is perhaps why simple shell models [9,20] also yield good estimates for  $\zeta_p$ .

In summary, then, we have shown that the RFNSE with  $y = 4$  exhibits the same multiscaling behavior as the 3DNSE, at least in the ESS sense. Probability distributions like  $P(\delta v_r)$  (Fig. 2c) are also qualitatively similar in the two models, in so far as they show deviations from Gaussian distributions for  $r$  in the dissipation range. It would be interesting to see if the RFNSE model can be obtained as an effective, inertial-range equation for fluid turbulence. We have tried to do this by a coarse-graining procedure that has been used [21] to map the Kuramoto–Sivashinsky (KS) equation onto the Kardar–Parisi–Zhang (KPZ) equation; however, it turns out that the 3DNSE  $\rightarrow$  RFNSE

mapping, if it exists, is far more subtle than the KS  $\rightarrow$  KPZ mapping as we discuss elsewhere [17].

We thank C. Das, A. Pande, S. Ramaswamy, and H. R. Krishnamurthy for discussions, CSIR (India) for support, and SERC (IISc, Bangalore) for computational resources.

\*Present address: Indian Institute of Foreign Trade, New Delhi, India.

†Also at Jawaharlal Nehru Centre for Advanced Scientific Research, Bangalore, India.

- [1] A. N. Kolmogorov, C.R. Acad. Sci. USSR **30**, 301 (1941).
- [2] For recent reviews, see K. R. Sreenivasan and R. Antonia, *Annu. Rev. Fluid Mech.* **29**, 435 (1997); S. K. Dhar *et al.*, Special issue on Nonlinearity and Chaos in Physical Sciences [*Pramana J. Phys.* **48**, 325 (1997)].
- [3] N. Cao, S. Chen, and K. R. Sreenivasan, *Phys. Rev. Lett.* **77**, 3799 (1996).
- [4] C. DeDominicis and P. C. Martin, *Phys. Rev. A* **19**, 419 (1979); D. Forster, D. R. Nelson, and M. J. Stephen, *Phys. Rev. A* **16**, 732 (1977).
- [5] V. Yakhot and S. A. Orszag, *Phys. Rev. Lett.* **57**, 1722 (1986); J. K. Bhattacharjee, *J. Phys. A* **21**, L551 (1988).
- [6] V. Yakhot, S. A. Orszag, and R. Panda, *J. Sci. Comput.* **3**, 139 (1988).
- [7] C. Y. Mou and P. B. Weichman, *Phys. Rev. Lett.* **70**, 1101 (1993).
- [8] G. L. Eyink, *Phys. Fluids* **6**, 3063 (1994).
- [9] S. K. Dhar, A. Sain, and R. Pandit, *Phys. Rev. Lett.* **78**, 2964 (1997).
- [10] R. Benzi *et al.*, *Phys. Rev. E* **48**, R29 (1993).
- [11] Z. S. She and E. Leveque, *Phys. Rev. Lett.* **72**, 336 (1994).
- [12] M. Meneguzzi and A. Vincent, in *Advances in Turbulence 3*, edited by A. V. Johansson and P. H. Alfredsson (Springer, Berlin, 1991), pp. 211–220.
- [13] For analogous studies of the randomly forced Burger’s equation, see A. Chekhlov and V. Yakhot, *Phys. Rev. E* **51**, 2739 (1995); F. Hayot and C. Jayaprakash, *Phys. Rev. E* **54**, 4681 (1996).
- [14] N. Cao, S. Chen, and Z. S. She, *Phys. Rev. Lett.* **76**, 3711 (1996).
- [15] U. Frish, *Turbulence: The Legacy of A. N. Kolmogorov* (Cambridge University Press, Cambridge, England, 1995).
- [16] Thus at the level of  $\Pi_k$  it seems that  $y_c = 4$ , but, as noted above, this value of  $y_c = 4$  does not emerge from our data for  $\zeta_p/\zeta_2$  ( $p \geq 3$ ) and  $P(\delta v_r)$ .
- [17] A. Sain and R. Pandit (unpublished).
- [18] E. D. Siggia, *J. Fluid Mech.* **107**, 375 (1981); Z. S. She, E. Jackson, and S. A. Orszag, *Nature (London)* **344**, 226 (1990).
- [19] S. Douady, Y. Couder, and M. E. Brachet, *Phys. Rev. Lett.* **67**, 983 (1991).
- [20] D. Pisarenko *et al.*, *Phys. Fluids A* **5**, 2533 (1993).
- [21] C. Jayaprakash, F. Hayot, and R. Pandit, *Phys. Rev. Lett.* **71**, 12 (1993).